Supplementary Information (SI) for Physical Chemistry Chemical Physics.
This journal is © the Owner Societies 2024

Supplementary Information

Intrinsic ultralow lattice thermal conductivity in lead-free halide perovskites $Cs_3Bi_2X_9$ (X = Br, I)

Jiang-Jiang Ma,‡[a] Jing-Jing Zheng,‡[b] Yuxi Chen,[a] Qingyong Ren,[cde] Junfeng Zhang[af*] and Bao-Tian Wang[cdg*]

[a] *School of Physics and Information Engineering, Shanxi Normal University, Taiyuan 030031, China;*
[b] *Department of Physics, Taiyuan Normal University, Jinzhong, 030619, China;*
[c] *Institute of High Energy Physics, Chinese Academy of Sciences (CAS), Beijing 100049, China;*
[d] *Spallation Neutron Source Science Center, Dongguan 523803, China;*
[e] *Guangdong Provincial Key Laboratory of Extreme Conditions, Dongguan, 523803, China;*
[f] *College of Physics and Electronic Engineering, Hainan Normal University, Haikou 571158, China;*
[g] *Collaborative Innovation Center of Extreme Optics, Shanxi University, Taiyuan, Shanxi 030006, China*

1. The formulas for mechanical properties

(i) The mechanical stability criteria for the Rhombohedral (I) systems of $Cs_3Bi_2Br_9$ written as:

$$\begin{aligned} &C_{11} > |C_{12}|, \quad C_{44} > 0, \\ &C_{13}^2 < \frac{1}{2} C_{33}(C_{11} + C_{12}), \\ &C_{14}^2 < \frac{1}{2} C_{44}(C_{11} - C_{12}) \equiv C_{44} C_{66} \end{aligned} \tag{S1}$$

(ii) The mechanical stability criteria for the hexagonal systems of $Cs_3Bi_2I_9$ written as:

$$\begin{aligned} &C_{11} > |C_{12}|, \\ &2C_{13}^2 < C_{33}(C_{11} + C_{12}), \\ &C_{44} > 0, \quad C_{66} > 0, \end{aligned} \tag{S2}$$

(iii) For rhombohedral crystal, the upper and lower bounds of bulk modulus are defined as:

$$\begin{aligned} &\mathrm{B_v} = \frac{1}{9}(2C_{11} + C_{33} + 2C_{12} + 4C_{13}), \\ &B_R = (2C_{11} + C_{33} + 2C_{12} + 4C_{13})^{-1}. \end{aligned} \tag{S3}$$

The upper and lower shear modulus are defined as:

$$\begin{aligned} &\mathrm{G_v} = \frac{1}{15}(2C_{11} + C_{33} - C_{12} - 2C_{13} + 6C_{44} + 3C_{66}), \\ &G_R = 15(8C_{11} + 4C_{33} - 4C_{12} - 8C_{13} + 6C_{44} + 3C_{66}). \end{aligned} \tag{S4}$$

(iv) For hexagonal crystal, the upper and lower bounds of bulk modulus and shear modulus are defined as:

$$
\begin{aligned}
\mathrm{B_v} &= \frac{1}{9}(2(C_{11}+C_{12})+4C_{13}+C_{33}),\\
B_R &= C^2/M,\\
G_V &= \frac{1}{30}(M+12C_{44}+12C_{66}),\\
G_R &= \frac{5}{2}[C^2C_{44}C_{66}]/[3B_VC_{44}C_{66}+C^2(C_{44}+C_{66})],\\
M &= C_{11}+C_{12}+2C_{33}-4C_{13},\\
C^2 &= (C_{11}+C_{12})C_{33}-2C_{13}^2.
\end{aligned}
\tag{S5}
$$

(v) The bulk modulus (B) and shear modulus (G) for are calculated from the Voigt-Reuss-Hill (VRH) approximations as follows:

$$
\mathrm{B}=\frac{1}{2}(B_v+B_R),\ \mathrm{G}=\frac{1}{2}(G_v+G_R) \tag{S6}
$$

The Young's modulus (E) are calculated through:

$$
\mathrm{E}=\frac{9BG}{3B+G} \tag{S7}
$$

(vi) The Poisson radio (υ), Debye temperature Θ_D (K) and Grüneisen parameter (γ) are calculated following relationships:

$$
\upsilon=\frac{1\text{-}2\left(v_t/v_l\right)^2}{2\text{-}2\left(v_t/v_l\right)^2} \tag{S8}
$$

where v_t is the transverse wave velocity, v_l is the longitudinal wave velocity.

$$
\theta_{\mathrm{D}}=\frac{h}{k_B}\left[\frac{3N}{4\pi V}\right]^{1/3}v_m \tag{S9}
$$

where h is Planck's constant, k_B is the Boltzmann constant, N is the number of atoms in a unit cell, V is the unit-cell volume, and v_m is the average phonon velocity, respectively.

$$
\gamma=\frac{3}{2}\left(\frac{1+\upsilon}{2-3\upsilon}\right) \tag{S10}
$$

where υ is Poisson's ratio.

2. The formula for participation ratio

The participation ratio (PR) is used to analyze the localized nature of the phonon mode. The PR value is defined as follow [1, 2]:

$$
PR(\omega_q)=\frac{(\sum_{i=1}^{N}\frac{\left|e(i,\omega_q)^2\right|}{M_i})^2}{N\sum_{i=1}^{N}\frac{\left|e(i,\omega_q)^4\right|}{M_i^2}} \tag{S11}
$$

where $e(i,\omega_q)$ are the phonon polarization vectors and M_i are the masses of the atoms.

Table S1. The Wyckoff positions fractional, partial charges and volume for atoms in $Cs_3Bi_2Br_9$ and $Cs_3Bi_2I_9$.

Materials	Atoms	Wyckoff Positions fractional			Partial charge	Bader volume
		x	y	z		
$Cs_3Bi_2Br_9$	Br(6i)	0.84	0.16	0.34	-3.30	41.0
	Br(3e)	0.50	0.00	0.00	-1.86	39.5
	Bi(2d)	0.33	0.67	0.81	+2.60	22.5
	Cs(2d)	0.33	0.67	0.34	+1.70	41.2
	Cs(1a)	0.00	1.00	0.00	+0.86	41.9
$Cs_3Bi_2I_9$	I(12*k*)	0.16	0.32	0.92	-5.93	51.4
	I(6*h*)	0.49	0.99	0.25	-3.07	51.1
	Bi(4*f*)	0.33	0.67	0.66	+3.99	24.9
	Cs(4*f*)	0.33	0.67	0.07	+3.33	43.3
	Cs(2*b*)	0.00	0.00	0.25	+1.68	43.4

Table S2. Calculated lattice constants a (Å) and c (Å) for $Cs_3Bi_2Br_9$ and $Cs_3Bi_2I_9$. The other experimental values are also listed for comparison.

Materials	Space group	Method	a&b (Å)	c (Å)
$Cs_3Bi_2Br_9$	P-3m1 (164)	EXP [3]	7.972	9.867
		EXP [4]	7.969	9.858
		PBE	8.194	10.110
		PBEsol	7.925	9.816
		DS-PAW	7.925	9.816
$Cs_3Bi_2I_9$	$P6_3/mmc$ (194)	EXP [5]	8.404	21.183
		EXP [6]	8.416	21.200
		PBE	8.637	22.213
		PBEsol	8.342	21.315
		DS-PAW	8.342	21.311

To balance the adequate calculation accuracy against the finite computational resources, we employed the PBE and PBEsol functional for structure optimization in VAPS code. Using PBE overestimates the lattice constants, while PBEsol underestimates them. In comparison, the calculations with PBEsol yield results that are closer to the experimental values of lattice constants. The crystal structure optimization is also verified using DS-PAW software [7], as shown in Table S1. The optimized lattice constants are in the best agreement with the experimental and theoretical values.

Table S3. Calculated bond length and the values of -ICOHP for $Cs_3Bi_2Br_9$ and $Cs_3Bi_2I_9$.

Materials	Bond	Bond length (Å)	-ICOHP (eV)
$Cs_3Bi_2Br_9$	Bi-Br1	2.741	-2.864
	Bi-Br2	2.953	-1.547
	Cs1-Br1	3.909	-0.257
	Cs2-Br1	4.026	-0.236
	Cs2-Br2	3.962	-0.249
$Cs_3Bi_2I_9$	Bi-I1	2.963	-2.196
	Bi-I2	3.199	-1.162
	Cs1-I1	4.060	-0.265
	Cs2-I1	4.286	-0.209
	Cs2-I2	4.172	-0.250

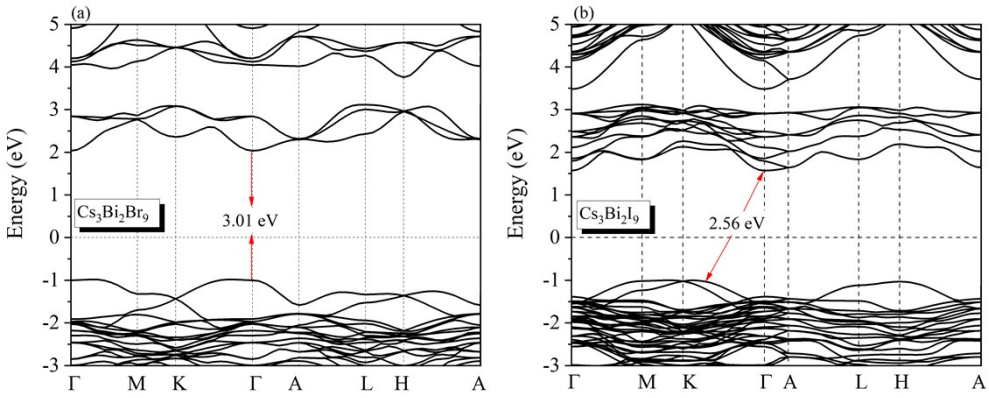

Fig. S1 Electronic band structures of (c) $Cs_3Bi_2Br_9$ and (d) $Cs_3Bi_2I_9$.

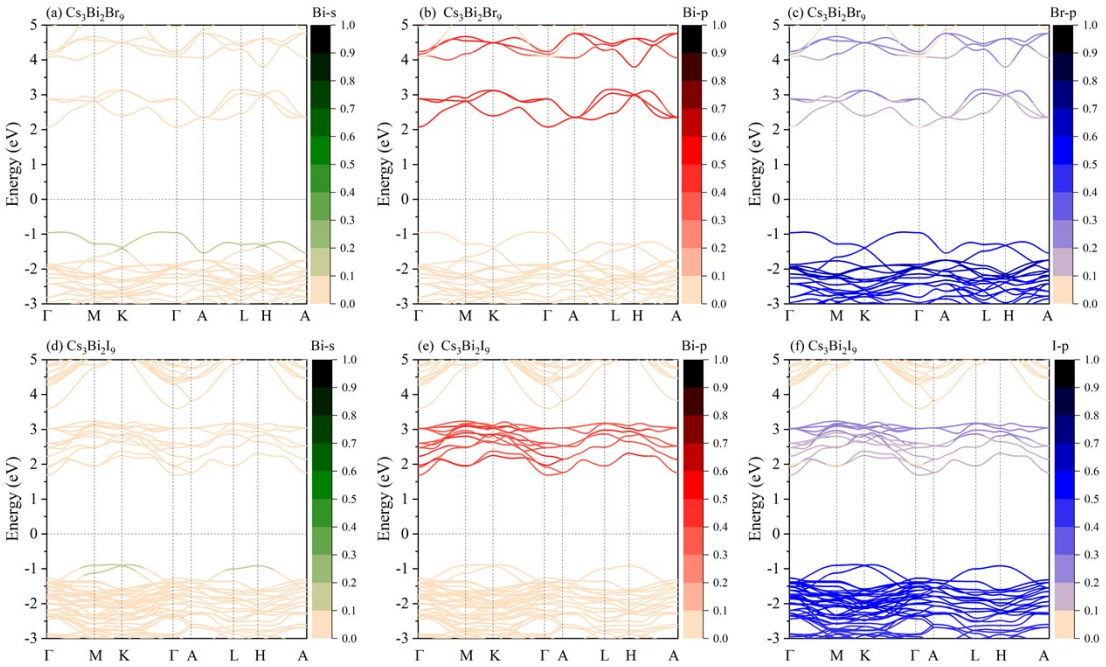

Fig. S2 The orbital-projected band of (a) Bi-s, (b) Bi-p, (c) Br-p and (d) Bi-s, (e)Bi-p, (I) I-p for $Cs_3Bi_2Br_9$ and $Cs_3Bi_2I_9$, respectively.

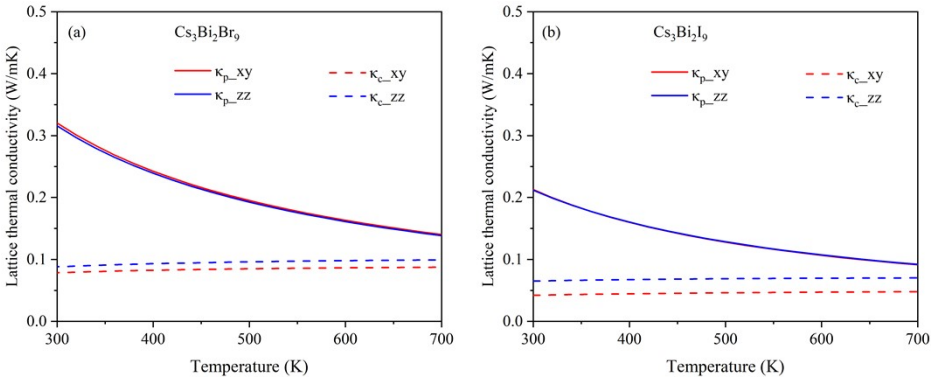

Fig. S3 Calculated lattice thermal conductivity for (a) $Cs_3Bi_2Br_9$ and (b) $Cs_3Bi_2I_9$ as a function of temperature along xy and z directions. The κ_P and κ_C are the particle-like and glass-like contribution for lattice thermal conductivity, respectively.

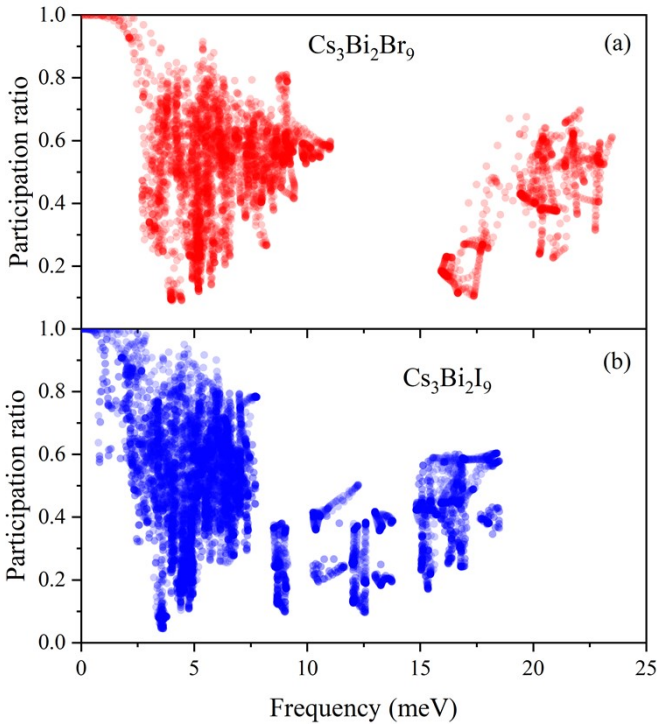

Fig. S4 The calculated participation ratios for the $Cs_3Bi_2Br_9$ and $Cs_3Bi_2I_9$

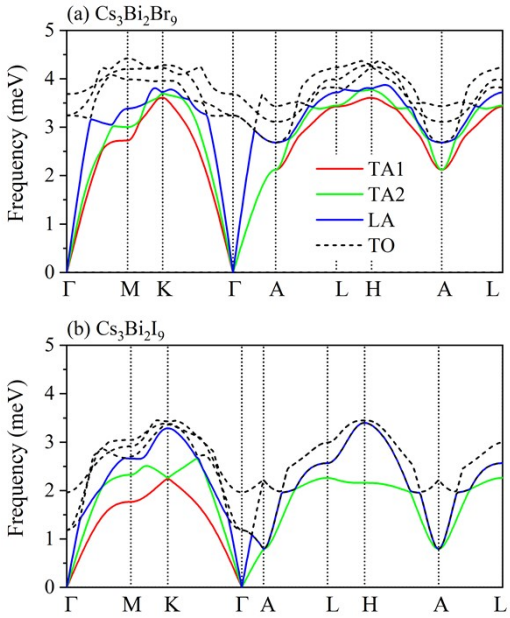

Fig. S5 The dispersion curves of acoustic modes and three low-lying optical modes for (a) $Cs_3Bi_2Br_9$ and (b) $Cs_3Bi_2I_9$, respectively.

References

[1] J. Hafner, M. Krajci. J Phys-condens Mat., 1993, **5**, 2489.

[2] P. Norouzzadeh, C. W. Myles, D. Vashaee. Phys Rev B, 2017, **95**, 195206.

[3] F. Lazarini. Acta Crystallogr B Struc. Sci. Cryst. Eng. Mater., 1977, **33**, 2961.

[4] D. Samanta, P. Saha, B. Ghosh, S.P. Chaudhary, S. Bhattacharyya, S. Chatterjee, G.D. Mukherjee. J Phys. Chem. C, 2021, **125**, 3432.

[5] A. Jorio, R. Currat, D. Myles, G. McIntyre, I. Aleksandrova, J. Kiat, P. Saint-Grégoire. Phys. Rev. B 2000, **61**, 3857.

[6] A.J. Lehner, D.H. Fabini, H.A. Evans, C.-A. Hébert, S.R. Smock, J. Hu, H. Wang, J.W. Zwanziger, M.L. Chabinyc, R. Seshadri. Chem. Mater. 2015, **27**, 7137.

[7] P.E. Blöchl. Phys. Rev. B, 1994, 50, 17953.